# Measurement of Depth-dependency and Anisotropy of Ultrasound Speed of Bovine Articular Cartilage *In Vitro*

Patil SG[1], Zheng YP[1], Wu JY[2], and Shi J[1]

[1] Rehabilitation Engineering Center, The Hong Kong Polytechnic University, Kowloon, Hong Kong SAR, China

[2] Department of Applied Biology and Chemical Technology, The Hong Kong Polytechnic University, Kowloon, Hong Kong SAR, China

Short Running Title: **Sound Speed of Articular Cartilage**

Corresponding Author:

Dr. Yongping Zheng

Rehabilitation Engineering Center

The Hong Kong Polytechnic University

Kowloon, Hong Kong SAR

China

Tel: 852 276676674

Fax: 852 23624365

Email: htzheng@polyu.edu.hk

Submitted to: Ultrasound in Medicine and Biology.

First submitted in July 2003.
Revised version submitted in April 2004

# Measurement of Depth-dependency and Anisotropy of Ultrasound Speed of Bovine Articular Cartilage *In Vitro*


## Abstract

The inhomogeneous and anisotropic mechanical properties and structural components of articular cartilage (AC) may cause complex acoustic properties in this important tissue. In this study, we used 50 MHz ultrasound to measure *in vitro* the depth-dependence and anisotropy of the ultrasound speed of AC collected from the bovine patellae. The ultrasound speeds of 18 disk AC specimens sampled from 18 different patellae were measured in two orthogonal directions. One full-thickness layer (n = 18) and three horizontal slices (n = 18*3) with approximately equal thickness were prepared from each AC disk and measured with the ultrasound beam perpendicular to the AC surface. One full thickness vertical slice (n = 10) was measured at different depths with the ultrasound beam parallel to the AC surface. The measured ultrasound speeds of AC in the two orthogonal directions were significantly different ($p < 0.001$). The ultrasound speeds also significantly increased with the increase of tissue depth for both measurement directions ($p < 0.001$). The ultrasound speeds of AC from the superficial to deep regions were 1518±17 (Mean + SD), 1532±26 and 1554±42 m/s for the ultrasound beam parallel to the AC surface, and 1574±29, 1621±34 and 1701±36 m/s for the beam perpendicular to the AC surface. The sound speed of the full-thickness layer was 1636±25 m/s. The results suggested that the depth-dependency and anisotropy of the ultrasound speed in AC should be taken into account when ultrasound is used for the AC measurement. It was also demonstrated in this study using additional specimens (5*2) that the swelling of AC after detaching from its subchondral bone could cause the change of its sound speed.



***Key Words:*** ultrasound speed, high-frequency ultrasound, articular cartilage, cartilage biomechanics, osteoarthritis, cartilage degeneration

## Introduction

Articular cartilage (AC) is a biphasic biological soft tissue that covers the end of articulating bones within synovial joints. It mainly consists of an organic composite matrix filled with liquids. Structurally, the organic composite matrix of AC can be regarded as a proteoglycan gel reinforced by a network of fine collagen fibrils and swollen with a multi-ionic electrolytic aqueous solution (Mankin et al. 1994; Mow et al. 1991). The biomechanical properties of AC are mainly determined by the organic composite matrix and its interactions with the liquid phase. Functionally, AC serves mainly as load bearing tissue in joints to carry high stresses and plays essential roles in joint lubrication (Kempson 1980; Mow et al. 1991). Fig. 1 illustrates the three zones of AC and the dimensional distribution of collagen over its full thickness. The volumetric concentration of collagen fibres increases from the superficial to deep zone (Langsjo et al. 1999). It is well accepted that collagen and proteoglycans of AC establish its tensile property and the compressive stiffness, respectively (Armstrong and Mow 1982; Harkness 1968; Kempson et al. 1973; Laasanen et al. 2003a). Due to the spatial variation of the water content, the proteoglycan concentration and the orientation of the collagen fibrils, the mechanical properties of AC are different at different depths. Therefore, AC is referred as structurally inhomogeneous and exhibits anisotropic mechanical properties. Wu and Herzog (2001) reported that the orientations of the collagen fibres and chondrocytes were responsible for the anisotropic mechanical property AC. Some studies reported the anisotropy of AC in compression (Jurvelin et al. 1996; Koehler et al. 2001; Wang et al. 2003). Measuring the depth-dependent properties of AC is important not only for the investigation of AC structure but also for finding the reason behind its degeneration as well as for the tissue engineering of AC (Risbud and Sittinger 2002).

The change of AC thickness has been widely used as an indicator to its degeneration status. The tissue thickness is also an important parameter for the measurements of the modulus of AC using indentation (Hayes et al. 1972). The thickness of AC was conventionally measured using calibrated microscopes (Jurvelin et al. 1995; Myers et al. 1995), micrometer installed with microscopes (Modest et al. 1989), and needling techniques (Jurvelin et al. 1995; Swann and Seedhom 1989; Toyras et al. 1999; Yao and Seedhom 1999). Most of the above techniques can only be used *in-vitro*. The AC thickness can also be measured *in-vivo* using MRI (McGibbon 2003) and X-ray (Buckland-Wright et al. 1995; Adam et al. 1998).

Recently, ultrasound techniques have been widely used for the measurement of AC thickness with a high resolution. In addition, ultrasound has been used to facilitate the measurement of biomechanical properties of AC using indentation or compression tests (Chen and Sah 2000; Fortin et al. 2003; Laasanen et al. 2002; 2003b; Macirowski et al. 1994; Mann et al. 2001; Nieminen et al. 2002; Rushfeldt et al. 1981; Toyras et al. 2001; Youn and Suh 2001; Zheng et al. 1998; 2001; 2002). Despite of the wide use of ultrasound in the morpholigical and biomechanical assessment of AC, ultrasound propagation in AC has not been well understood, particularly for its depth-dependency and anisotropy.

The sound speed in AC is an important parameter for the measurement of AC thickness using ultrasound (Adam et al. 1998; Lefebvre et al. 1998; Modest et al. 1989; Rushfeldt et al. 1981; Saied et al. 1997; Toyras et al. 2001). Constant ultrasound speeds were frequently used in these studies based on the values reported in the literature. Yao and Seedhom (1999) reported a very large variation of ultrasound speed of human AC. In their study, the thickness was measured using the needling technique. The accuracy of the sound speed measurement might be affected

by the mismatch of the exact measurement site or direction for the needle punching and ultrasound reflection. Suh et al. (2001) measured the ultrasound speed and thickness of AC tissues simultaneously *in situ* by applying an indentation on the AC surface. Using this technique, the ultrasound speed of AC could be measured without the knowledge of AC thickness. Since the stiffness of AC tissues significantly depends on the depth (Guilak et al. 1995; Schinagl et al. 1996; Wang et al. 2002; Zheng et al. 2001; 2002), AC is compressed non-uniformly during indentation. Thus the knowledge about the depth-dependence of ultrasound speed of AC is critical to this new approach.

The sound speed may vary in AC due its heterogeneous structure through its depth. Agemura et al. (1990) measured sections of bovine AC prepared both parallel and perpendicular to the AC surface using a scanning laser acoustic microscope with an ultrasound frequency of 100 MHz. Their preliminary study with two specimens demonstrated that the ultrasound speed of AC tissue measured with the ultrasound beam parallel to the AC surface varied with its depth. In the present study, we investigated the depth-dependent and anisotropic behaviors of the AC using a non-contact ultrasound method, which measured the sound speed and thickness of the specimen simultaneously. Similar methods have been used to obtain the sound speeds of various engineering materials (Kuo et al. 1990; Hsu and Hughes 1992).

## Materials and Methods

### *Experimental Setup*

A schematic representation of the experimental setup is shown in Fig. 2. A focused ultrasound transducer (Model PI50-2, Panametrics, Waltham, MA USA) with

a nominal frequency of 50 MHz, a focal zone diameter (-6 dB) of 0.1 mm, and a focal length of 12.8 mm was fixed to a positioning stage (Model R301MMX, Deltron Precision Inc., Bethel, CT). The ultrasound transducer could be translated vertically in one dimension with a precision of 0.01 mm. The specimen was installed on a pair of plates and secured by two elastic threads to prevent potential movements during the test. Three pairs of this arrangement were contained in a saline bath which could be translated in two horizontal directions with a precision of 0.01 mm via a positioning stage (Model 2201MMXY, Deltron Precision Inc., Bethel, CT). The focus of the ultrasound transducer was located approximately at the middle of the specimen.

The ultrasound transducer was driven by an ultrasound pulser/receiver (Model 5601A, Panametrics, Waltham, MA USA). The received ultrasound signals were digitized by an A/D converter (CompuScope 8500PCI, Gage, Canada) at a sampling rate of 500 MHz, and stored in the PC for offline signal analysis (Zheng and Mak 1996; Zheng et al. 2002). The pulser/receiver settings, including the transmitting energy, receiving gain, attenuation and damping were selected according to pilot experiments and were maintained during the course of the experiments.

*Specimen Preparation*

Twenty-three fresh mature bovine patellae without any surface damage were harvested within 6 h of death and stored in a refrigerator at -20°*C* prior to sectioning. It has been reported that cryopreservation (Kiefer et al 1989), freezing and thawing (Agemura et al 1990; D'Astous and Foster 1986; Kim et al 1995) of specimens would not affect the mechanical and acoustic properties such as ultrasound speed, attenuation and backscatter of AC. Specimen preparation was carried out by excising the lateral part of the patella, and then separating it into two pieces by cutting perpendicular to the articular surface. An AC slab with a bone layer approximately 5

mm thick was prepared from each piece, and 6.35 mm plugs were cored out from the flat area of slab using a metal punch as shown in Fig. 3. The samples were kept moist with normal saline solution during preparation. One specimen from the upper right quadrant of each patella was tested in this study after further preparations described as follow.

Three different categories of AC slices were prepared from 18 disks in the second phase of specimen preparation (Fig. 4). A thin surgical blade was used manually to excise a small portion of AC with a width of approximately 2 mm for full-thickness measurement (n = 18). A lateral vertical slice with a width of approximately 1 mm was then prepared (n = 10), and the AC surface was marked as an indicator for this block. The remaining portion of the AC was cut into three horizontal slices (n = 18*3) parallel to the AC surface, each of approximately equal thickness. These three groups of specimens were then used for the ultrasound measurement within 15 minutes after the preparation.

The remaining 5 disks were prepared to investigate the swelling effects of AC after the specimens were detached from the bone. The AC disks were first thawed in saline for at least 2 h before further preparation. A full-thickness slice was first excised from each disk and installed onto the specimen platform for measurement with the ultrasound beam perpendicular to the AC surface. The procedure for the specimen preparation and installation was completed within 1 min. After the test of this specimen, another full-thickness AC specimen was prepared from the same AC disk. The procedure was similar as that of the first full-thickness slice, however the AC slice was obtained from the diametrically opposite direction of the disk to avoid the potential effects caused by the previous cut. This specimen was installed with the ultrasound beam parallel to the AC surface.

*Measurement Procedure*

***Slice Measurement for Sound Speed.*** The vertical slice and full-thickness slices were first placed on the plates in the container. The superficial layer of the full-thickness slice was arranged to face the ultrasound beam. In the case of vertical slice it was made sure that the superficial layer was scanned first followed by the middle and deep layers with the ultrasound beam parallel to the AC layers. The ultrasound beam was first located approximately 2 mm away from the edge of the first AC specimen and ultrasound signal reflected from the bottom of the container was collected. Then the ultrasound transducer was moved horizontally towards the specimen in 0.25 mm intervals and a total of eight sites on the container bottom were measured. The ultrasound beam was then moved to pass through the vertical slice specimen and ultrasound signals were recorded at intervals of 0.05 mm. The collected ultrasound signals included echoes from the upper and lower surfaces of the specimen, and the bottom of the container. As shown in Fig. 4, the ultrasound beam was scanned along the vertical cutting interface of the AC specimen and measurements were made on a number of sites located from the superficial layer to the deep layer. The position of each measurement site was recorded from the micrometer screw gauge. After the ultrasound beam passed the specimen region, ultrasound signals were collected from the gap between the vertical slice and the full-thickness slice at intervals of 0.25 mm. Similarly, ultrasound signals from the full-thickness slice were collected at a distance of 0.05 mm. Beyond the full-thickness specimen, ultrasound signals were recorded again at eight sites on the bottom of the container with 0.25 mm intervals. Three scans were performed across each specimen at a distance of 0.5 mm (Fig 4).

The horizontal AC slices with the cut parallel to the AC surface were measured in a similar way. Three slices from a single specimen were placed on the three pairs of plates in the container. The ultrasound beam was scanned along the container bottom at equal intervals of 0.25 mm and along the specimens at equal intervals of 0.05 mm. An example of the ultrasound reflections from the upper and lower surfaces of the specimen and the surface of the container base is shown in Fig. 5.

***Baseline Drift Amendment.*** The perpendicular orientation of the ultrasound beam to the container bottom is important for accurate measurements. To ensure the uniformity of the distance from the transducer to the container bottom at different scanning sites, the baseline of the container bottom was first carefully adjusted before the measurement. In addition, further correction was made by using the ultrasound echoes reflected directly from the bottom of the container on the measurement sites and beyond the AC specimens. A pair of tracking cursors was used to track the shift of the echoes reflected from the bottom of the container directly or passing through the AC specimen. Since the horizontal positions of the measurement sites were recorded with the micrometer screw gauge, a linear regression between the position and the flight time shift was made for the measurement sites without the presence of AC specimen. The regression line represented the slope of the container bottom and was used to correct the flight time of the echoes reflected from the bottom of the container for the measurement sites on the AC specimen.

***Calculation of Ultrasound Speed in Saline and AC.*** Ultrasound reflections were collected by a program in real time and were analyzed offline. As shown in Fig. 5, three pairs of tracking windows were used to track the signals reflected from the interfaces of the specimen and the container. Each tracking cursor could be moved

individually with a time resolution of 2 ns as defined by the sampling rate (500 MHz) of the A/D converter. In this study, cross-correlation of the ultrasound echoes was used as references for the measurement of flight time *T*. Two corresponding full cycles of RF signal were marked by the tracking windows on the echoes reflected from two interfaces of AC slices, respectively. Fig. 6 shows a schematic representation for the ultrasound paths and flight times involved in the calculation of the ultrasound speeds. $T_1$, $T_2$, and $T_3$ represent the flight times of the round trips of ultrasound from the transducer to the interfaces of the upper surface of the AC slice, the lower surface of AC slice, and the bottom of the container through the specimen. $T_4$ represents the round trip from the bottom of the container without the presence of the specimen. The ultrasound speed in the saline solution was measured by moving the transducer vertically down by two steps of 0.5 mm and then back to the original position in two steps. $T_5$ represents the position of the transducer after it is moved from its original position. The difference between the flight times obtained at the four positions was used to calculate the ultrasound speed in the saline solution as follow:

$$c_w = \frac{2d_T}{(T_4 - T_5)} \tag{1}$$

where $c_w$ is the ultrasound speed in saline, $d_T$ was the vertical distance traveled by the transducer. An average value of the speed in the saline solution calculated for all the steps was used for the further calculation of the ultrasound speed in AC.

The ultrasound speed in AC was calculated as follows (Refer to Fig. 6):

$$\frac{T_3}{2} = \frac{d_{ab}}{c_w} + \frac{d_{bc}}{c_{AC}} + \frac{d_{cd}}{c_w} \tag{2}$$

$$\frac{T_4}{2} = \frac{d_{ab}}{c_w} + \frac{d_{bc}}{c_w} + \frac{d_{cd}}{c_w} \tag{3}$$

*Also*

$$\frac{T_1}{2} = \frac{d_{ab}}{c_w} \tag{4}$$

$$\frac{T_2}{2} = \frac{d_{ab}}{c_w} + \frac{d_{bc}}{c_{AC}} \tag{5}$$

$$\frac{d_{cd}}{c_w} = \frac{T_3}{2} - \frac{T_2}{2} \tag{6}$$

$d_{ab}$, $d_{bc}$, and $d_{cd}$ represent the distance between the transducer and the specimen upper surface, the specimen thickness, and the distance between the specimen lower surface and the surface of the container base, respectively. By substituting eqns (4) and (6) into eqns (2) and (3), we get:

$$d_{bc} = \left( \frac{T_2}{2} - \frac{T_1}{2} \right) * c_{AC} \tag{7}$$

$$\frac{T_4}{2} = \frac{T_1}{2} + \frac{d_{bc}}{c_w} + \frac{T_3}{2} - \frac{T_2}{2} \tag{8}$$

By further substituting eqn (7) into eqn (8), we get:

$$c_{AC} = \frac{T_4 - T_3 + T_2 - T_1}{T_2 - T_1} * c_w \tag{9}$$

$$d_{AC} = c_{AC} * \frac{T_2 - T_1}{2} \tag{10}$$

where $c_{AC}$ is the ultrasound speed in the AC tissue and $d_{AC}$ is the thickness of AC slice.

***Measurement for Swelling Effects.*** It was a concern whether the sound speed of AC would change as a function of time due to swelling effects after it was detached from its subchondral bone. The two full-thickness slices prepared from each of the 5

patellae were immediately installed onto the specimen platform and monitored for 1 h with the ultrasound beam parallel and perpendicular to the AC surface, respectively. The monitoring site was located at approximately the middle of the surface facing the ultrasound beam. The transient thickness and sound speed of the AC specimen were calculated using the method introduced in the last section, where $T_4$ in eqn (9) was measured after the specimen was removed from the specimen platform.

***Data Analysis.*** The ultrasound speeds measured at the various sites, along the three scanning lines were averaged to obtain a mean value for the full-thickness and horizontal slices. This averaged value was used for the further data analysis of the superficial, middle and deep slices. For the vertical slice, the ultrasound speeds measured at different sites along a scanning line was equally separated into three groups representing superficial, middle and deep regions. The ultrasound speeds of the measurement sites of each region were averaged, and the result was further averaged with those obtained along the other two scanning lines.

Two-factor ANOVA (SPSS v11.0.0, SPSS Inc., Chicago, US) was used to test the significance of the differences in ultrasound speeds measured for the three horizontal slices and the three regions of the vertical slices. Both the region dependence and the orientation dependence of the ultrasound speed in AC tissues were tested. In order to test the reproducibility of the technique, the sound speeds measured along the three scan lines (0.5 mm apart) for each slice were compared using intra-class correlation (SPSS v11.0.0, SPSS Inc., Chicago, US). The mean of the percentage standard deviation for the three measurements of each slice was also calculated as an indicator for reproducibility.

## Results

The reproducibility test showed the sound speed measured along the three different scanning lines for each slice agreed well with a mean percentage standard deviation of 2.2%. The intra-class correlation coefficient for 95% confidence level was $r = 0.9721$ ($p < 0.001$), which showed a very high reproducibility.

The mean thickness (+SD) of the superficial, middle and deep horizontal slices ($n = 18*3$) were $0.64 \pm 0.18$ mm, $0.50 \pm 0.18$ mm, and $0.59 \pm 0.18$ mm, respectively. The mean thickness for the full-thickness layers ($n = 18$) was $1.64 \pm 0.30$ mm, which was slightly smaller than the sum of the three slices ($1.73 \pm 0.31$ mm). The increase (5.5%) of the summed thickness of the slices was possibly due to the AC swelling after slicing. This swelling issue would be further discussed in the following sections.

The ultrasound speeds of AC tissues at the superficial, middle and deep regions were $1518 \pm 17$ m/s (Mean $\pm$ SD), $1532 \pm 26$ m/s and $1554 \pm 42$ m/s with the ultrasound beam parallel to the AC surface ($n = 18$), and $1574 \pm 29$ m/s, $1621 \pm 34$ m/s and $1701 \pm 36$ m/s with the beam perpendicular to the AC surface ($n = 10$) (Fig. 7). The ultrasound speeds of AC tissue significantly increased from the superficial to middle and deep regions for both measurement directions (ANOVA, $p<0.001$). The ultrasound speeds of AC measured in the two orthogonal directions were significantly different (ANOVA, $p<0.001$). There was a quadratic relationship ($R^2 = 0.9982$) between the ultrasound speed and the tissue depth for the measurements of the vertical slices (Fig. 8). The error bars in Fig. 8 represents the standard deviation among the results of the 10 specimens. The variation among the specimens as shown in Fig. 8 was similar to those in Fig. 7, though the scale was changed in Fig. 8 better to represent the quadratic relationship. The sound speed increased from 1518 m/s to 1559 m/s (2.7%) when the measurement region moved from the most superficial to

the deepes zone of the AC layer. The sound speed of the full-thickness AC layer (n = 18) was 1636±25 m/s (ranged from 1598 m/s to 1721 m/s).

It was demonstrated that there was an increasing trend for the AC thickness for both measurement directions for the 5 specimens tested (Fig. 9a). No distinguished difference was noted between the results measured in the two directions. Hence the results shown in Fig. 9a were the combined data of all the 10 slices from the 5 specimens. This change of the AC thickness was believed to be caused by the swelling effect of AC due to its excision from the subchondral bone. Most of the increase in thickness was observed within the first 5 min. At time points 1, 15, 30 and 60 min, the mean increases of the thickness were summarized in Table 1. The AC thickness changed by 3.6% after 15 min. It appeared that the measurement performed at 15 min was just slightly different in comparison with that performed at 60 min (changed by 0.2%). Large variations among specimens were observed. Considering the results of individual specimens, most of them showed different degrees of increase but few of them showed slight decrease as time going.

The sound speed results showed similar but smaller increasing trend in comparison with that of AC thickness (Fig. 9b). No distinguished difference was observed for the changes of the sound speed between the results obtained in two different directions. Most of the changes also happened within 5 min. At time points 1, 15, 30 and 60 min, the mean increases of the sound speed were also summarized in Table 1. The sound speed changed by 1.2% after 15 min. It appeared that the measurement made at 15 min were just slightly different in comparison with that made at 60 min (changed by 0.2%). Considering the results of individual specimens, majority of them showed different degrees of increase but some of them showed decrease as time going.

## Discussion

This paper reported a study of the depth-dependent and anisotropic behavior of ultrasound speed in bovine patellar AC. It was demonstrated that the ultrasound speed of AC significantly depended on the tissue depth. The ultrasound speed measured with the ultrasound beam parallel and perpendicular to the AC surface both increased from the superficial to the deep layer. The ultrasound speed measured with the beam perpendicular to the AC surface (overall mean for different depths 1629±71 m/s) (Mean + SD) was significantly larger than that measured with the beam parallel to the AC surface (1535±18 m/s). Similar results have been reported previously with fewer specimens (Agemura et al 1990). The increasing trends of ultrasound speed in both directions might be related to depth dependent mechanical properties and structural components of AC. Similarly, the anisotropic behavior of the sound speed in AC might be due to the anisotropic mechanical properties and micro-structures of AC (Kempson et al. 1980, Mow et al. 1991, Mankin et al. 1994). The ultrasound speed of the full-thickness AC was 1636+25 m/s, which was within the similar range of the averaged ultrasound speed of the three horizontal slices (1629+71 m/s). The sound speed measured in the present study with the 50 MHz ultrasound beam perpendicular to the AC surface and under room temperature was within the similar range as reported in most of the previous studies for bovine and human cartilages. The sound speeds of full-thickness AC reported in the previous studies have been summarized in Table 2. It was noted that most of the ultrasound speed of AC reported in the literature was measured under either room temperature or 37°C. The effects of temperature on the ultrasound speed measurement of AC deserve to be further studied.

It was noted that the waveforms of the ultrasound echo would distort for different degrees as it propagates through the AC specimen. This distortion was caused by the AC's frequency-dependent attenuation (Joiner et al. 2001) and possibly nonlinear acoustic properties (Zheng et al. 1999). In this study, a cross-correlation algorithm was used to measure the time-of-flight of the ultrasound signal in AC by matching the RF wave of the echoes reflected from different interfaces. The distortion of the echoes could potentially affect the cross-correlation matching (Ragozzino 1981). High correlations ($R^2$ >0.9) between the echoes were achieved for most of the specimens in this study. When the waveforms were significantly distorted, the echoes to be matched were first manually located and the cross-correlation approach was then used to optimize the matching.

The theoretical relationship between the longitudinal ultrasound speed and mechanical parameters is shown in eqn (11).

$$c = \sqrt{(K + 4/3G)/\rho} \tag{11}$$

where $c$ is the longitudinal ultrasound speed, $K$ is the bulk modulus, $G$ is the shear modulus, and $\rho$ is the density of the material (Stanley 1968). Eqns (12) and (13) provide the relationship between the bulk modulus $K$, shear modulus $G$, Young's modulus $E$, and Poisson's ratio $\nu$ of an isotropic material (Mow et al 1991).

$$K = \frac{E}{3(1-2\nu)} \tag{12}$$

$$G = \frac{E}{2(1+\nu)} \tag{13}$$

It has been reported that the Young's modulus of AC tissues increased from superficial layer to the deep layer (Guilak et al. 1995; Laasanen et al. 2003a; Schinagl et al. 1996; Wang et al. 2002; Zheng et al. 2002). The increasing trend of the ultrasound speed of AC at depths from the AC surface to the bone appeared to agree

with increasing trend of equilibrium Young's modulus. Recently, Laasanen et al. (2003a) reported that the middle region of the bovine knee AC had much larger Poisson's ratio (up to 0.4) in compression as compared to the superficial and deep regions (low to 0.1). Wang et al. (2003) demonstrated that the equilibrium compressive moduli of AC were significantly different when measured in different directions. Their results showed that modulus of the superficial region measured with the compressing direction perpendicular to the AC surface was significantly smaller than that measured with the compression in other two orthogonal directions. However, the deep region of AC showed a reversed feature. Due to the complexity of mechanical properties of AC, it appears that the correlation between the anisotropy and depth-dependence of the equilibrium compressive modulus of AC and its longitudinal ultrasound speed was not so straightforward. In addition to Young's modulus and Poisson's ratio the contents of the fluid phase and the shear modulus of AC are not constant from the superficial region to the deep region (Athanasiou et al. 1991). Even though there are few studies reported on the density of AC (Joseph et al. 1999), it is reasonable to predict that AC density is also depth-dependent considering the depth-dependent water contents and other components. Considering the variations of these parameters, it appears difficult to have a simple relationship between the depth-dependent Young's modulus and the ultrasound speed.

Another difficulty is that material properties obtained in conventional mechanical tests could not be directly used for eqn (11). According to the AC density (1050 kg/m3) reported by Joseph et al. (1999), the instantaneous Young's modulus (8.5 MPa, Laasanen et al. 2003, measured with 2 mm/s compression rate for 10% deformation), and the instantaneous Poisson's ratio of 0.4 for bovine patellar AC (Fortin et al. 2003, measured with a 2 s ramp compression); the sound speed

calculated using eqn (11) is only 132 m/s. This value was much smaller than that measured in the present and all the previous studies. The main reason might be that AC is a viscoelastic (biphasic poroelastic) material so that it is difficult to measure its real instantaneous modulus and Poisson's ratio, which is involved in the acoustic wave propagation as well as in eqn (11). The compression rate for measuring the instantaneous modulus and Poisson's ratio as reported is much smaller as compared with that happens in the ultrasonic wave. In other words, the real instantaneous modulus of AC should be much larger than those reported in the literature. Other factors like anisotropy and inhomogeneity of AC might also affect the result in using eqn (11).

Toyras et al. (2003) reported that the ultrasound speed of full-thickness AC significantly depends on the equilibrium Young's modulus, water content and other AC composition. Agemura et al. (1990) reported that the differences in ultrasound speed among different regions of AC to its dissimilar fibril organization. In the superficial, middle and deep region, the collagen fibers are parallel, random and perpendicularly oriented to the surface of the AC, respectively (Mankin et al. 1994; Mow et al. 1991). Agemura et al. (1990) concluded with a limited number of specimens that the ultrasound appeared to propagate faster across the long axis of collagen fibrils than along them. In the present study the measured ultrasound speed significantly increased from the superficial region to the deep region. A study with fine slice preparation is necessary to further clarify the correlation between the collagen fibril orientation and the ultrasound speed in AC.

Previous studies have suggested that detaching the AC from its subchondral bone could cause swelling and curling of the specimen (Myers et al. 1984; Setton et al. 1998). We concluded from the results of the swelling tests that the swelling effects

after detaching should be taken into account during the measurement of the AC sound speed and thickness. It was noted that the change of the speed of sound was minor (1.2% at 15 min after detaching from the bone) but not negligible considering the small changes caused by the variations of tissue depth and measurement directions. The sound speed increased by 3.0% and 5.0% from the superficial to deep layer with the ultrasound beam perpendicular to the AC surface; increased by 1.0% and 1.4% with the beam parallel to the AC surface; and decreased by 6.2% when the measurement direction was changed from perpendicular to parallel orientation to the AC surface. In comparison with the variation of the sound speed among specimens, the variation of sound speed caused by the detaching was found to be much larger. The reasons for this large variation should be further studied together with the other issues such as the variation during the period of 1 min while the specimen was detached from bone and installed on the specimen holder.

It is obvious that the swelling effects to the sound speed should be taken into account when AC is detached from the bone, particularly for the measurement with the ultrasound beam parallel to the AC surface, where the change of the sound speed as a function of tissue depth was relatively small. In spite of the fact that our results of the depth- and orientation-dependent ultrasound speed might be affected by the swelling effects explained above, they should still have reference values considering the fact that majority of the sound speed measurement previously reported were based on specimens detached from the subchondral bone. In addition, it appears that measuring in-situ depth- or orientation-dependent ultrasound speed is still difficult using available technology. More systematic studies on swelling effects are suggested so that the outcome may benefit the field of ultrasonic and biomechanical measurements of AC. Our preliminary results using 5 pairs of specimens

demonstrated that there was no obvious difference between the swelling effects measured in two orthogonal directions. This finding should be supported by tests on a larger number of specimens. The tissue depth may play an important role for the swelling, as AC has depth-dependent composition, structure and mechanical property. This issue should be addressed in the future studies. Without this information, the conclusion of the depth-dependency of the sound speed of AC obtained in the present study can be applicable to the AC specimens detached from the subchondral bone. The depth-dependency of the swelling-induced change of the sound speed in AC is not yet evident and requires further investigations.

In summary, the anisotropy and depth-dependency of the sound speed of AC was investigated in this study for bovine patella specimens detached from the subchondral bone using a noncontact ultrasound method that could obtain the speed of sound and tissue thickness simultaneously. This noncontact measurement could be very useful for accurate measurement of AC thickness and sound speed in future ultrasonic studies for AC. The anisotropic nature of AC tissue was demonstrated as the ultrasound speeds of AC measured in the two orthogonal directions were significantly different. The ultrasound speeds of AC significantly increased from the superficial to deep layers for both measurement directions. The influences of the depth-dependent swelling effects to the depth-dependency of the sound speed in AC need to be further studied. This study suggests that the depth-dependence and anisotropy of ultrasound speed in AC tissues should be taken into account in the studies for ultrasound characterization of AC. Although the measurements in the present study were made on the normal bovine patellar AC, the results should be also applicable for human AC because of their similar structure and biomechanical properties. In the ultrasonic measurement of sound speed and thickness of AC

specimens, their orientations relative to the ultrasound beam should be carefully marked and the measured AC zones should be documented. In cases of in-situ or in-vivo measurement or imaging of the non-uniform mechanical or acoustic properties of AC using ultrasound, the effect of depth-dependent sound speed should be compensated or discussed.

**Acknowledgements**

This work was partially supported by the Research Grants Council of Hong Kong (PolyU5199/02E) and The Hong Kong Polytechnic University (G-T468).

**References:**

Adam C, Eckstein F, Milz S, et al. The distribution of cartilage thickness in the knee-joints of old-aged individuals – measurement by A-mode ultrasound. Clinical Biomechanics. 1998; 13: 1-10.

Agemura DH, O'Brien WD, Olerud JE, Chun LE, and Eyre DE. Ultrasonic propagation properties of articular cartilage at 100 MHz. Journal of Acoustic Society of America. 1990; 87: 1786-1791.

Armstrong CG and Mow VC. Variation in intrinsic mechanical property of human articular cartilage with age, degeneration and water content. Journal of Bone Joint Surgery. 1982; 64: 88-94.

Athanasiou KA, Rosenwasser MP, Buckwalter JA, Malinin TI, and Mow VC. Interspecies comparison of in situ intrinsic mechanical properties of distal femoral cartilage. Journal of Orthopaedic Research. 1991; 9: 330-340.

Buckland-Wright JC, Macfarlane DG, Lynch JA, Jasani MK, and Bradshaw CR. Joint space width measures cartilage thickness in osteoarthritis of the knee: High resolution plain film and double contrast macroradiographic investigation. Annuals of the Rheumatic Diseases. 1995; 54: 263-268.

Chen AC and Sah RL. Deformation of articulating cartilage: Ultrasound analysis. Proceedings of 46th Annual meeting Orthopedics Research Society. 2000; 0887: 12-15.

D'Astous FT and Forster FS. Frequency dependence of ultrasound attenuation and backscatter in breast tissue. Ultrasound in Medicine and Biology. 1986; 12: 795-808.

Fortin M, Buschmann MD, Bertrand MJ, Foster FS, and Ophir J. Dynamic measurement of internal solid displacement in articular cartilage using ultrasound backscatter. Journal of Biomechanics. 2003; 36: 443-447.

Guilak F, Ratcliffe A, and Mow VC. Chondrocyte deformation and local tissue strain in articular cartilage: A Confocal microscopy study. Journal of Orthopaedic Research. 1995; 13: 410-421.

Harkness RD. Mechanical properties of collagen tissues. In: Gould BS, ed. Biology of Collagen 2. New York: London, Academic Press. 1968: 247-310.

Hayes WC, Keer LM, Herrmann G, and Mockros LF. A mathematical analysis of indentation tests of articular cartilage. Journal of Biomechanics. 1972; 5: 541-51.

Hsu DK and Hughes MS. Simultaneous ultrasound velocity and sample thickness measurement and application in composites. Journal of Acoustic Society of America. 1992; 92: 669-675.

Joiner GA, Bogoch ER, Pritzker KP, et al. High frequency acoustic parameters of human and bovine articular cartilage following experimentally-induced matrix degradation. Ultrasonic Imaging. 2001; 23: 106-116.

Joseph D, Gu WY, Mao XG, Lai WM, and Mow VC. True density of normal and encymatically treated bovine articular cartilage. Proceedings of 45th Annual Meeting of Orthopaedic Research Society, Feb 1999, Anaheim, CA, US. p642.

Jurvelin JS, Rasanen, Kolmonen P, and Lyyra T. Comparison of optical, needle probe and ultrasonic techniques for the measurement of articular cartilage thickness. Journal of Biomechanics. 1995; 28: 231-235.

Jurvelin JS, Buschmann MD, and Hunziker E. Mechanical anisotropy of human knee articular cartilage in compression. Transaction of Orthopaedic Research Society 1996; 21: 340–347.

Kempson GE, Muir H, Pollard C, and Tuke M. The tensile property of cartilage of human femoral condyles related to contents of collagen and glycosaminoglycans. Biochimica et Biophysica Acta. 1973; 297: 456-472.

Kempson GE. The mechanical properties of articular cartilage. In: Sokoloff L, ed. The Joints and Synovial Fluid, vol. II. New York: Academic Press. 1980; 177-238.

Kiefer GN, Sundby K, McAllister D, et al. The effect of Cryopreservation on the biomechanical behaviour of bovine articular cartilage. Journal of Orthopaedic Research. 1989; 7: 494-501.

Kim HK, Babyn PS, Harasiewicz KA, and Foster FS. Imaging of immature articular cartilage using ultrasound backscatter microscopy at 50Mhz. Journal of Orthopaedic Research. 1995; 13: 963-970.

Koehler T, Szeri AZ, and Buchanan TS. An inhomogeneous, anisotropic spring model of articular cartilage. 25th Annual Meeting of the American Society of Biomechanics. 2001; 118.

Kuo IK, Hete B, and Shung KK. A novel method for the measurement of acoustic speed. Journal of Acoustic Soceity of America. 1990; 88: 1679-1682.

Laasanen MS, Toyras J, Hirvonen J et al. Novel mechano-acoustic technique and instrument for diagnosis of cartilage degeneration. Physiological Measurement. 2002; 23: 491-503.

Laasanen MS, Toyras J, Korhonen RK et al. Biomechanical properties of knee articular cartilage. Biorheology. 2003a. 40: 133-140.

Laasanen MS, Toyras J, Vasara AI et al. Mechano-Acoustic diagnosis of cartilage degenration and repair. The Journal of Bone and Joint Surgery. 2003b; 85-A Suppl 2: 78-84.

Langsjo TK, Hyttinen M, Pelttari A, et al. Electron microscopic stereological study of collagen fibrils in bovine articular cartilage: Volume and surface densities are best obtained indirectly (from length densities and diameters) using isotropic uniform random sampling. Journal of Anatomy. 1999; 195: 281-93.

Lefebvre F, Graillat N, Cherin E, Genevieve B, and Saied A. Automatic three dimensional reconstruction and charaterization of articualr cartilage from high-resolution ultrasound acquisitions. Ultrasound in Medicine and Biology. 1998; 24: 1369-1381.

Macirowski T, Tepic S, and Mann RW. Cartilage stresses in the human hip joint. Journal of Biomechanical Engineering. 1994; 116: 10-18.

Mankin HJ, Mow VC, Buckwalter JA, Iannotti JP, and Ratcliffe A. Form and function of articular cartilage. In: Simnon SR, ed. Orthopaedic Basic Science. American Academy of Orthopaedic Surgeons,.1994; 2-44.

Mann RW, Shepherd DET, and Seedhom BB. Discussion on: A technique for measuring the compressive modulus of articular cartilage under physiological loading rates with preliminary results. Proc Instn Mech Engrs: J Engr Medicine. 2001; 215:123-124.

McGibbon CA. Inter-rater and intra-rater reliability of subchondral bone and cartialge thickness measurement from MRI. Magnetic Resonance Imaging. 2003; 21: 707-714.

Modest VE, Murphy MC, and Mann RW. Optical verification of a technique for in situ ultrasonic measurement of articular cartilage thickness. Journal of Biomechanics. 1989; 22: 171-176.

Mow VC, Zhu W, and Ratcliffe A. Structure and function of articular cartilage and meniscus. In: Mow VC, and Hayes WC, ed. Basic Othopaedic Biomechanics. New York: Raven Press. 1991; 143-198.

Myers ER, Lai WM, and Mow VC. A continuum theory and an experiment for the ion-induced swelling behavior of articular cartialge. Journal of Biomechanical Engineering. 1984; 106: 151-158.

Myers SL, Dines K, Brandt DA, Brandt KD, and Alvrecht ME. Experimental assessment by high frequency ultrasound of articular cartilage thickness and osteoarthritic changes. Journal of Rheumatology. 1995; 22: 109-116.

Nieminen HJ, Toyras J, Rieppo J, et al. Real-time ultrasound analysis of articular cartilage degradation in vitro. Ultrasound in Medicine and Biology. 2002; 28: 519-525.

Pellaumail B, Watrin A, Loeuille D, et al. Effect of articular cartilage proteoglycan depletion on high frequency ultrasound backscatter. Osteoarthritis in Cartilage. 2002; 10: 535-541.

Ragozzino M. Analysis of the error in measurement of ultrasound speed in tissue due to waveform deformation by frequency-dependent attenuation. Ultrasonics. 1981; 19: 135-138.

Risbud MV and Sittinger M. Tissue engineering: advances in in-vitro cartilage generation. Trends in Biotechnology. 2002; 20: 351-356.

Rushfeldt PD, Mann RW, and Harris WH. Improved techniques for measuring in vitro geometery and presssure distribution in the human acetabulum: Ultrasonic measurement of acetabular surface, sphericity and cartilage thickness. Journal of Biomechanics. 1981; 14: 253-260.

Saied A, Cherin E, Gaucher H, et al. Assessment of articular cartilage and subchondral bone: subtle and progressive changes in experimental osteoarthritis using 50MHz echography in vitro. Journal of Bone and Mineral Research. 1997; 12: 1378-1386.

Schinagl RM, Ting MK, Price JH, and Sah RL. Video microscopy to quantitate the inhomogeneous equilibrium strain within articular cartilage during confined compression. Annals of Biomedical Engineering. 1996; 24: 500-512.

Setton LA, Tohyama H, and Mow VC. Swelling and curling behaviors of articular cartilage. Journal of Biomechanical Engineering. 1998; 120: 355-361.

Stanley RC. Light and Sound for Engineers. Hart Publishing Company, Inc. New York City. 1968; 251.

Suh JKF, Youn I, and Fu FH. An in situ calibration of an ultrasound transducer: a potential application for an ultrasonic indentation test of articular cartilage. Journal of Biomechanics. 2001; 34: 1347-1353.

Swann AC and Seedhom BB. Improved techniques for measuring the indentation and thickness of articular cartilage. Proceedings of Institution Mechanical Engineers. 1989; 203: 143-150.

Toyras J, Rieppo J, Nieminen MT, Helminen HJ, and Jurvelin JS. Characterization of enzymatically induced degradation of articular cartilage using high frequency ultrasound. Physics in Medicine and Biology. 1999; 44: 2723-2733.

Toyras J, Lyyra-Laitinen T, Niinimaki M, et al. Estimation of the Young's modulus of articular cartilage using an arthroscopic indentation instrument and ultrasound measurement of tissue thickness. Journal of Biomechanics. 2001; 34: 251-256.

Toyras J, Laasanen MS, Saarakkala S, et al. Speed of sound in normal and degenrated bovine articular cartilage. Ultrasund in Medicine and Biology. 2003; 29: 447-454.

Wang CCB, Deng JM, Ateshian GA, and Hung CT. An automated approach for direct measurement of two-dimensional strain distributions within articular cartilage under unconfined compression. Journal of Biomechanical Engineering. 2002; 124: 557-567.

Wang CCB, Chahine NO, Hung CT, and Ateshian GA. Optical determination of anisotropic material properties of bovine articular cartilage in compression. Journal of Biomechanics. 2003; 36: 339-353.

Wu JZ, Herzog W. Mechanical anisotropy of articular cartilage is associated with variations in microstructures. 24th Annual Meeting of the American Society of Biomechanics. 2001; 275.

Yao JQ and Seedhom BB. Ultrasonic measurement of thickness of human articular cartilage in situ. Rheumatology. 1999; 38: 1269-1271.

Youn I and Suh JK. Acoustic charateristics of collagen and glycosaminoglycan in articular cartilage. Proceedings of 47th Annual Meeting Orthopedics Research Society. 2001; 0435: 25-28.

Zheng YP and Mak AFT. An ultrasound indentation system for biomechanical properties assessment of soft tissues in vivo. IEEE Transactions on Biomedical Engineering. 1996; 43: 912-918.

Zheng YP, Mak AFT, Qin L, and Ding CX. Ultrasound elastography of articular cartilage: A preliminary study. Proceedings of 20th Annual International Conference of IEEE EMBS, Hong Kong. 1998: 1940-1942.

Zheng YP, Maev RG, and Solodov Iyu. Nonlinear acoustic applications for material characterization: a review. Canadian Journal of Physics. 1999; 77: 1-41.

Zheng YP, Ding CX, Bai J, Mak AFT, and Qin L. Measurement of the layered compressive properties of trypsin-treated articular cartilage: an ultrasound investigation. Medical and Biological Engineering and Computing. 2001; 34: 534-541.

Zheng YP, Mak AFT, Lau KP, and Qin L. Ultrasonic measurement for in-vitro depth-dependent equilibrium strains of articular cartilage in compression. Physics in Medicine and Biology. 2002; 47: 3165-3180.

## Figure Captions

**Fig. 1.** Schematic representation of the layered stucture of AC (Mow et al. 1991).

**Fig. 2.** Experimental setup for the measurement of the ultrasound speed of AC. The ultrasound transducer could be moved vertically to focus the ultrasound beam in the specimen. The specimen base could also be moved horizontally in two dimensions to locate different measurement points. The ultrasound signals were digitized, displayed in real-time, and stored in PC for further off-line analysis.

**Fig. 3.** Schematic representation of the procedure for the preparation of AC plugs of 6.35 mm diameter. The specimens would be further prepared for the measurement of the ultrasound speed of AC (Fig. 4).

**Fig. 4.** Schematic representation of the preparation of the AC cylinder into slice specimens for ultrasound measurements. The full-thickness slice was removed first. The vertical cutting separated the middle piece (vertical slice) used for the measurement with the ultrasound beam parallel to the AC surface. The remained larger piece was further cut into three pieces (horizontal slices) with approximately equal thickness and used for the measurement with the ultrasound beam perpendicular to the AC surface. The dots on each slice indicate the sites for the ultrasound measurement.

**Fig. 5.** Typical ultrasound echoes from interfaces. A cross-correlation technique was used to track the echoes. The echoes indicated by ‘c’ represents the reference signal and echoes indicated by ‘a’ and ‘b’ were located by the cross-correlation tracking. The echoes to be matched were overlapped with the reference echo in ‘a’ and ‘b’.

**Fig. 6.** Schematic representation for the elements involved in the calcuation of the ultrasound speed in AC and saline. $d_{AC}$ is the thickness of AC slice; $T_1$ to $T_5$ are the

flight times of the round trips of ultrasound from the transducer to different interfaces. $T_4$ is measured after a vertical movement of the transducer and used to calculate the ultrasound speed in the saline solution.

**Fig. 7.** Depth-dependent ultrasound speeds of AC tissues. The error bar represents the standard deviation. The vertical slice was measured with the ultrasound beam parallel to the AC surface, while the horizontal and full-thickness slices was measured with the beam perpendicular to the AC surface. Two-factor ANOVA demonstrated significant differences between the ultrasound speeds measured in two orthogonal directions and among different regions.

**Fig. 8.** Ultrasound speed measured in the vertical slice throughout the full thickness of AC. The presented data were the average of the ten specimens and the error bars indicated the standard deviations. It was demonstrated that the ultrasound speed was significantly dependent on the depth of AC.

**Fig. 9**. The changes of (a) normalized AC thickness and (b) normalized sound speed as a function of time after the specimen was detached from the bone. Ten full-thickness slice specimens were prepared from 5 disk specimens, which were cored from 5 different bovine patellae. The 2 slices from each disk specimens were tested in two different orthogonal directions, respectively. No distinguished difference was noted between the results measured in the two directions. Hence the results shown in the figure were the combined data of all the 10 slices from the 5 patellae.

# FIGURES

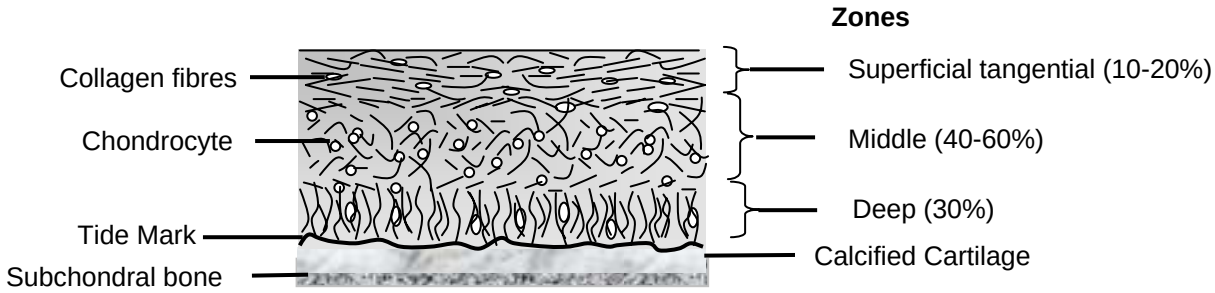


**Fig. 1**

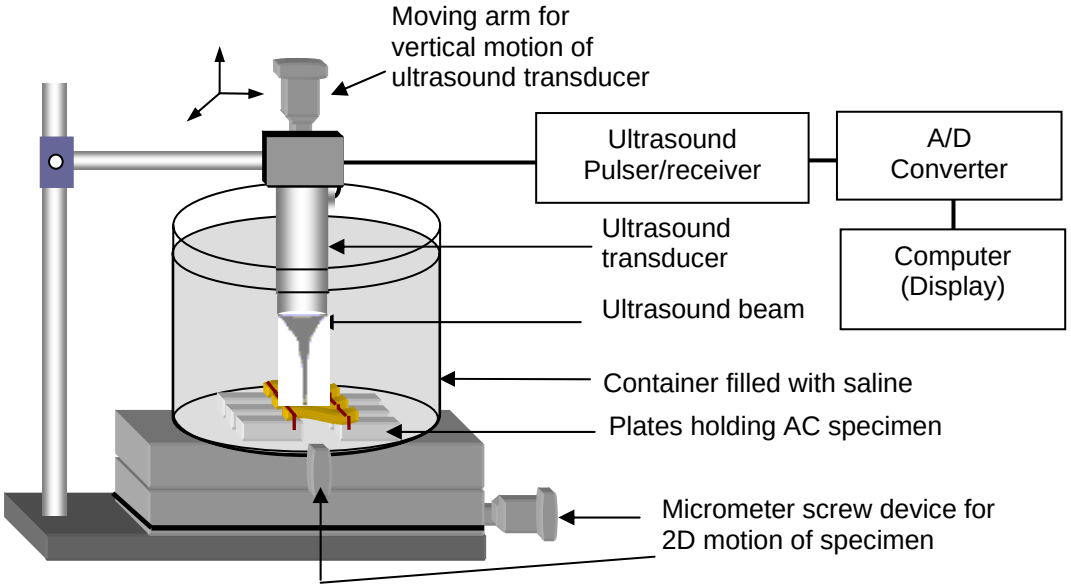


**Fig. 2**

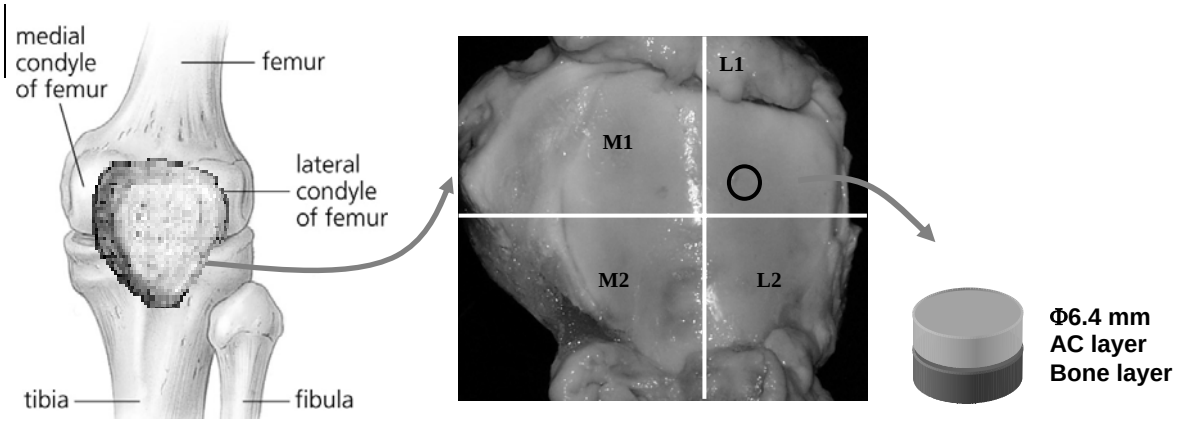


**Fig. 3**

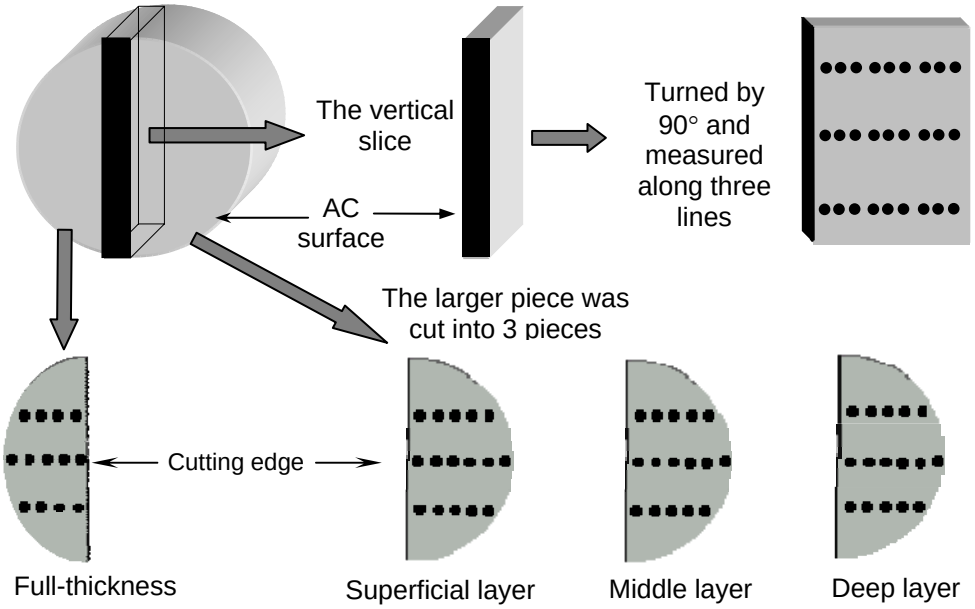
The vertical slice
AC surface
Turned by 90° and measured along three lines
The larger piece was cut into 3 pieces
Cutting edge
Full-thickness
Superficial layer
Middle layer
Deep layer

**Fig. 4**

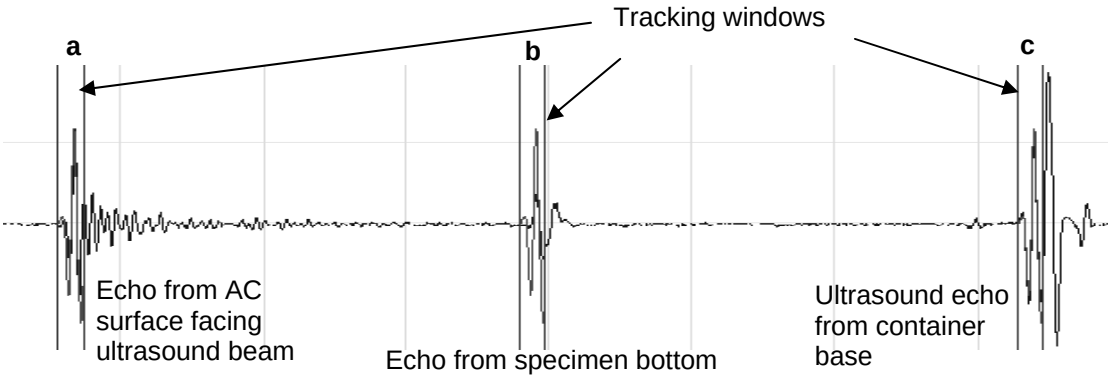
Tracking windows
a
b
c
Echo from AC surface facing ultrasound beam
Echo from specimen bottom
Ultrasound echo from container base

**Fig. 5**

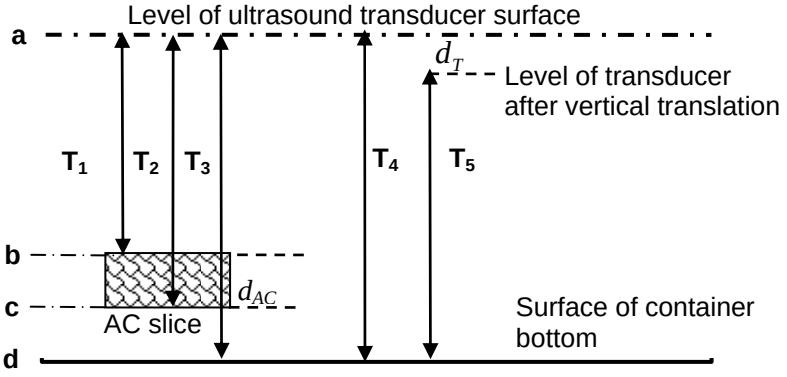
Level of ultrasound transducer surface
a
$d_T$
Level of transducer after vertical translation
$T_1$
$T_2$
$T_3$
$T_4$
$T_5$
b
c
$d_{AC}$
AC slice
Surface of container bottom
d

**Fig. 6**

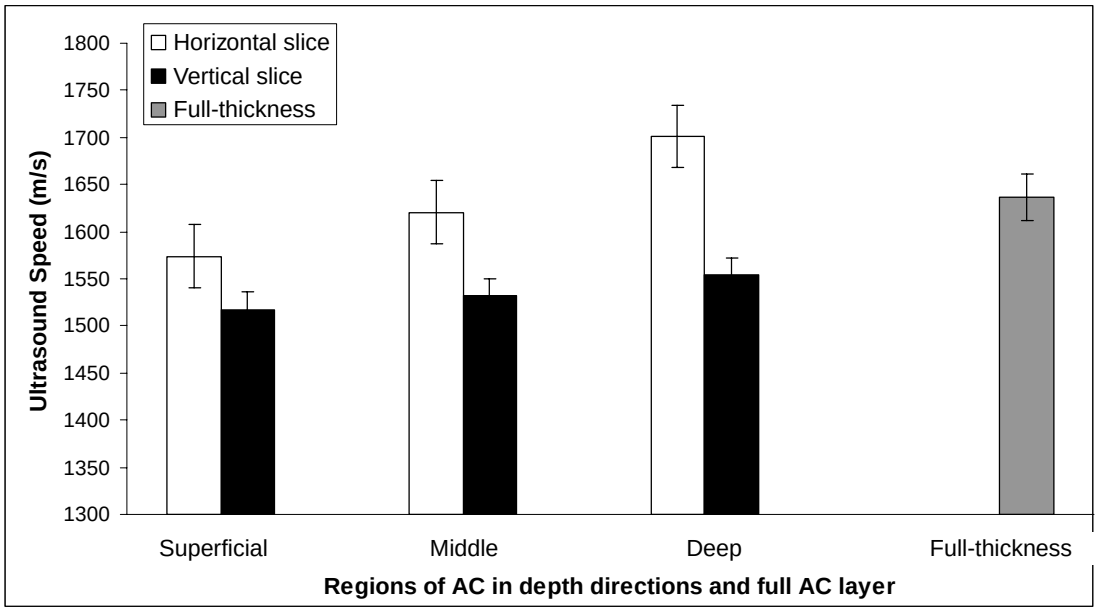


**Fig. 7**

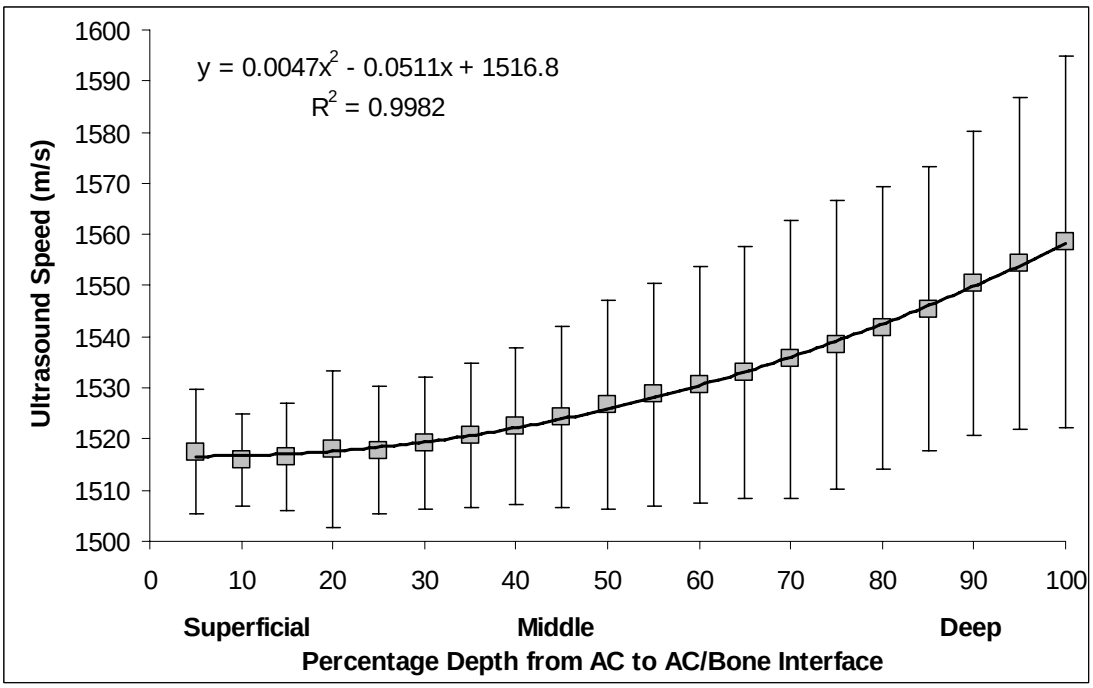


**Fig. 8**

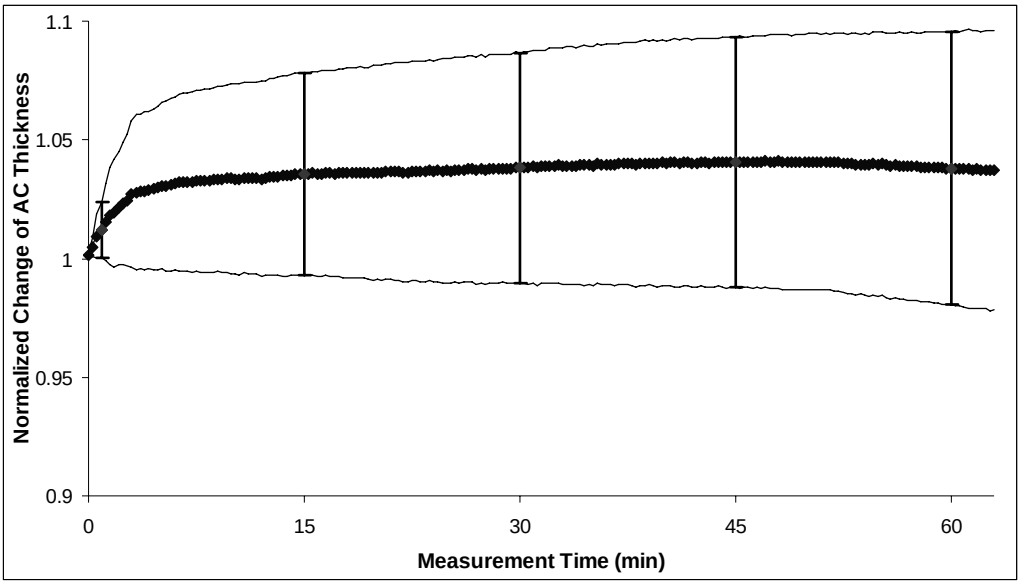
Normalized Change of AC Thickness
1.1
1.05
1
0.95
0.9
0
15
30
45
60
Measurement Time (min)

(a)

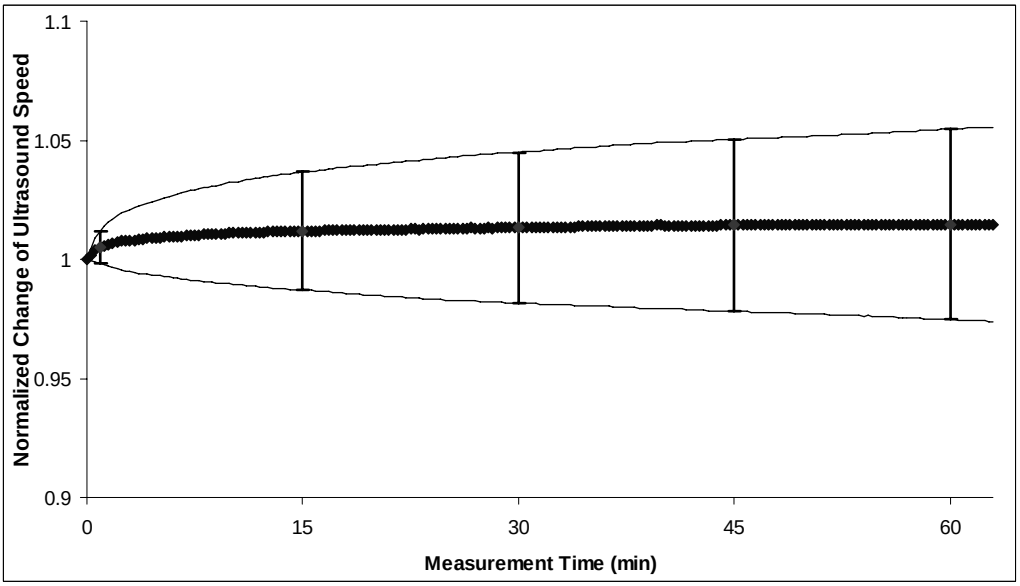
Normalized Change of Ultrasound Speed
1.1
1.05
1
0.95
0.9
0
15
30
45
60
Measurement Time (min)

(b)

**Fig. 9**

**Table 1.** The mean normalized sound speed and thickness of AC slice specimens measured at different time after they were detached from their subchondral bones and installed on the specimen platform (corresponding to Fig. 9). Ten full-thickness slice specimens were prepared from 5 disk specimens, which were cored from the approximately same location of 5 different bovine patellae. The 2 slices from each disk specimens were tested in two different orthogonal directions, respectively. The results obtained in the two directions were combined together in the table, as no significant differences were demonstrated due the change of the measurement direction.

| Time (min) | Normalized Speed | | Normalized Thickness | |
|---|---|---|---|---|
| | Mean | SD | Mean | SD |
| 1 | 1.005 | 0.007 | 1.012 | 0.012 |
| 15 | 1.012 | 0.025 | 1.036 | 0.043 |
| 30 | 1.013 | 0.032 | 1.038 | 0.049 |
| 45 | 1.014 | 0.036 | 1.041 | 0.053 |
| 60 | 1.014 | 0.040 | 1.038 | 0.058 |

**Table 2.** A summary of the sound speed of full-thickness AC reported in the literature. The information of the specimen type, ultrasound frequency, and testing temperature were included. In addition, the methods used for thickness measurement were also described.

| Authors (Year) | AC Specimen | Ultrasound frequency | Testing temperature | Thickness measurement | Sound speed |
|---|---|---|---|---|---|
| Modest et al. (1989) | Human femoral head | 7.5 MHz | Room temperature | Microscope and needle insertion | 1760 m/s |
| Jurvelin et al. (1995) | Canine and bovine femoral and tibial condyles | 10 MHz | Room temperature (22.5°C) | Microscope and needle insertion | 1760 m/s (verified) |
| Agemura et al. (1990) | Bovine patella | 100 MHz | Room temperature | Optical method | 1617 ~ 1720 m/s |
| Myers et al. (1995) | Human femoral condyle | 25 MHz | Room temperature | Microscope | 1658±185 m/s |
| Yao et al. (1999) | Human hip and ankle joint | 20 MHz | Room temperature | Needle insertion | 1892±183 m/s |
| Toyras et al. (1999) | Bovine patella | 22 MHz | 37°C | Needle insertion | 1654±82 m/s |
| Joiner et al. (2001) | Bovine femoral condyle<br>Human femoral condyle | 30 MHz | 37°C | Ultrasound propagation in saline with specimen in contact with the bottom | 1666±16 m/s<br>1664±7 m/s |
| Suh et al. (2001) | Bovine patellar and femoral condyle | 10 MHz | Room temperature | Microscope | 1735±35 m/s |
| Toyras et al. (2003) | Bovine femoral condyle, patella, patello femoral groove and talus joint | 10.3 MHz | Room temperature (20°C) | Microscope | 1627 m/s (1532 ~ 1754 m/s) |
| Present study | Bovine patella | 50 MHz | Room temperature (19.5 ± 1°C) | Ultrasound propagation in saline with specimen lifted | 1626±25 m/s |